Structural, Energetic, and Vibrational Properties of NO_x Adsorption on Ag_n, $n = 1-8$

Henrik Grönbeck,* Anders Hellman, and Andreas Gavrin

Department of Applied Physics and Competence Centre for Catalysis, Chalmers University of Technology, SE-412 96 Göteborg, Sweden

Received: February 9, 2007; In Final Form: May 8, 2007

The density functional theory is used to explore structural, electronic, and vibrational properties of NO, NO_2, and NO_3 adsorption on small silver clusters, Ag_n, with $n = 1-8$. Generally, NO adsorbs in atop configuration, whereas NO_2 and NO_3 are adsorbed in bridge configuration. NO_2 and NO_3 introduce pronounced structural relaxations in the clusters. In particular, the transition size from planar to three-dimensional structures is modified. For each cluster size, the adsorption energies follow the trend E_a (NO) < E_a (NO_2) < E_a (NO_3). The adsorption energies show a marked odd/even alternation with a stronger bonding to odd clusters. Analysis of the electronic structure reveals an ionic bond mechanism for NO_2 and NO_3. Odd/even effects are also present in vibrational properties of the adsorbed radicals. With respect to the gas phase, the largest shifts are calculated for adsorption on odd clusters. Possible implications of the results for Ag/Al_2O_3 HC-SCR catalysts are discussed.

I. Introduction

One of the main motivations for the study of gas phase atomic clusters is the possibility of novel chemical properties. Indeed, the pioneering experiments of cluster reactivity uncovered marked size variations.[1−3] For example, the reaction rate constants of H_2 with Fe_n was measured to change several orders of magnitude in the size range Fe_6 to Fe_{68}.[2] The observed changes were non-monotonic, and pronounced differences were observed from one cluster size to another. Because adsorption processes are influenced by both structural and electronic factors, the underlying reason for the size variations is a challenging issue. In the case of H_2 reactivity with Fe_n, the reactivity strongly correlates with the cluster ionization thresholds.[3] Clusters with a low ionization threshold were measured to react more efficiently with H_2 than clusters with a high threshold.

Following the early experiments,[1−3] cluster reactivity in the gas phase has been explored for several transition metals and reactions.[4] Moreover, it has been possible to investigate the size dependence of catalytic reactions such as CO and H_2 oxidation on Pt_n.[5,6] Clusters from the coinage metal group (Cu, Ag, and Au) have received special attention. The interest arises as these clusters show a regular and marked size variation in electronic properties, including ionization potentials and electronic affinities.[7] In addition to variations that correlate with electronic shell closings for delocalized electrons in an external potential,[8] this type of clusters exhibit odd/even alternations with respect to the number of atoms in the cluster.[7,9] Interestingly, similar size variations have been observed for chemical processes, such as O_2 reactivity and CO oxidation.[10]

In view of the large size-to-size variation in the reactivity of coinage metal clusters, it is intriguing that the active metal phase in the HC-SCR (selective catalytic reaction with hydro-carbons as the reducing agent) reaction of NO_x over an Ag/Al_2O_3 catalyst[11] has recently been proposed to be small Ag_n clusters.[12,13] By comparing UV−vis spectra for an Ag/Al_2O_3 catalyst with reference samples with known Ag_n sizes, it was concluded that the active clusters consist of less than eight atoms.[12] Moreover, *in situ* EXAFS (extended X-ray absorption fine structure spectroscopy) measurements revealed an average Ag−Ag coordination number of ∼2.7, which suggests clusters as small as trimers or tetramers.[13] Of course, because the clusters are small, it is probable that the support material (γ-alumina) influences the catalytic properties of the metal clusters. The complexity of adsorption on multicomponent systems have recently been demonstrated for molecular adsorption on metals supported on oxides (see, for example, refs 14−16) and oxides supported on metals.[17]

Owing to the interesting intrinsic properties of Ag_n clusters and in an attempt to increase the understanding of the metal phase in the HC-SCR Ag/Al_2O_3 catalyst for NO_x reduction, we have performed a systematic density functional theory (DFT)-based study of NO_x adsorption on gas-phase Ag_n clusters with $n \leq 8$. The sequence from NO to NO_3 was considered, and results are presented for structural and energetic as well as vibrational properties.

The adsorption of NO on transition metal clusters has previously been explored within DFT for Pd_1-Pd_6,[18] Fe_1-Fe_6,[19] Rh_6[20] and Cu_4, Ag_4, and Cu_2Ag_2.[21] These studies show that molecular NO is adsorbed preferably with N attached to the cluster. Moreover, NO is predicted to dissociate on Fe clusters larger than the monomer[19] and on Rh_6.[20]

II. Computational Methods

DFT[22,23] is applied with the gradient corrected exchange correlation functional according to Perdew, Burke, and Ernzerhof (PBE).[24] The one-electron Kohn−Sham orbitals are expanded in a localized numerical basis set.[25−27] A double numerical basis set is used together with polarization functions. A real space cutoff of 4.5 Å is used for the basis functions. A pseudo potential[28] is utilized for Ag to describe the interaction between the valence electrons ($4s^2 4p^6 4d^{10} 5s^1$) and the nucleus, together with the inner shell electrons. The Kohn−Sham equations are solved self-consistently using an integration technique based on weighted overlapping spheres centered at

* Corresponding author. E-mail: ghj@chalmers.se.

10.1021/jp071117d CCC: $37.00
Published on Web 06/19/2007

each atom. The direct Coulomb potential is obtained by projection of the charge density onto angular dependent weighting functions also centered at each atom. The Poisson equation is, thereafter, solved by one-dimensional integration.

The potential energy surfaces of the bare clusters and clusters with adsorbates are investigated by geometrical relaxation (without symmetry constraints) starting from several different configurations. For bare clusters larger than the tetramer, at least six different isomers were considered. All different atop and bridge sites were investigated for NO, NO_2, and NO_3 adsorption on relevant neutral and cationic cluster isomers. That the reported structures are minima are confirmed by calculations of the vibrational spectra. The vibrational analysis is performed via numerical derivatives.

As a reference, Ag in the bulk phase is considered. These calculations apply periodic boundary conditions, and reciprocal space integration over the Brillouin zone is approximated with a finite sampling using the Monkhorst−Pack scheme.[29,30]

III. Results and Discussion

Bare neutral and charged silver clusters in the size range discussed here have been the subject of numerous first principles investigations.[31−39] These studies have established the relevant isomers and, particularly, the transition from two-dimensional (2D) to three-dimensional (3D) motifs. For neutral clusters, the transition occurs between hexamer and heptamer, whereas for cations, the first size with 3D structure is Ag_5^+. For the positively charge clusters, the early structural transition has been supported by ion mobility measurements.[36] Because Ag clusters follow the trend for clusters with one valence electron, they are less complex than the Au counterparts, which were shown to be 2D over a wider size range[40,41] owing to the delocalization of *d*-electrons.[42]

In this section, we start by presenting results for bare neutral and cationic clusters. Although these systems already have been thoroughly discussed in the literature, this provides an opportunity to evaluate the quality of the computational technique. Moreover, the properties of the bare clusters are essential to understand the results for NO_x adsorption. NO, NO_2, and NO_3 adsorption will be discussed in the subsequent section.

A. Bare Neutral and Cationic Clusters. Results for bare and cationic cluster structures are presented in Figure 1, together with point group determination and energetic properties. For the neutral clusters, only the stable isomers are reported. Two isomers of Ag_8 have similar stability. Instead of reviewing literature data of Ag_n isomers, we refer to the review in ref 35.

The spectroscopic constants of the dimer are calculated to 1.71 eV (binding energy), 2.61 Å (bond distance), and 179 cm^{-1} (vibrational wavenumber). These results compare favorably with previous DFT reports using the same functional.[40] In ref 40, where a plane-wave pseudo potential method was used, the binding energy and bond distance were reported to be 1.62 eV and 2.63 Å, respectively. The corresponding experimental values are 1.66 eV,[43] 2.53 Å,[44] and 192 cm^{-1}.[43]

The stable isomer of the trimer is the obtuse iso-scaled triangle. The angle is in this case 75°. The acute (55°) isomer is calculated to be 0.07 eV above the ground state. The structures for Ag_4 to Ag_6 are formed by decorating the triangle with one to three caps. These geometries are all planar. For the hexamer, the second best isomer (0.25 eV above the reported isomer) is a pentagonal pyramid, which is 3D. The stable heptamer is a pentagonal bi-pyramid. Thus, this structure is based on the second best geometry for Ag_6. The ground state of the octamer

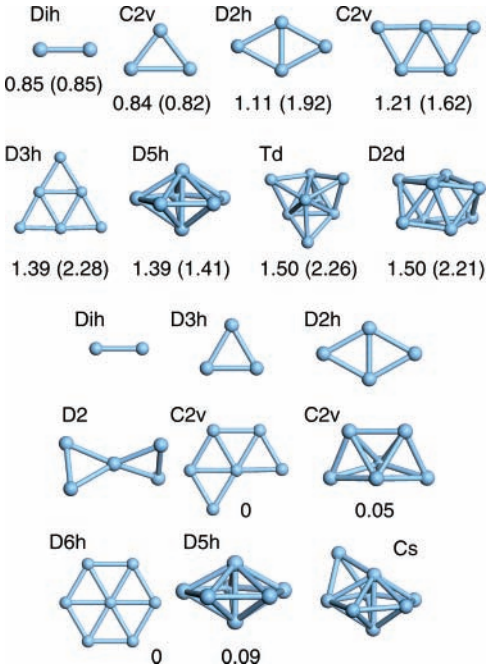

Figure 1. Structural models of low energy isomers of neutral (top) and cationic (bottom) clusters. The symmetry point group is indicated. For the neutral clusters, the cohesion energy is reported together with the monomer fragmentation energy (in parentheses). For Ag_n^+ clusters with the same size, the relative ordering is reported. All energies are in eV.

is calculated to be a tetra-capped tetrahedron, which has T_d symmetry. This structure is preferred by 0.05 eV over the dodecahedron (D_{2d}). The present results concerning relevant ground-state structures are in agreement with previous DFT reports.[35,38] The average bond distances for the ground-state clusters increase monotonically with cluster size and range from 2.61 Å for the dimer to 2.85 Å for the T_d isomer of Ag_8. As expected, the bonds in these small clusters are contracted with respect to the nearest neighbor distance in the bulk, which in the present approach is calculated to be 2.99 Å. The experimental value is 2.89 Å.[45]

The cohesion energy of the clusters (Figure 1) is clearly reduced with respect to the bulk value, which is calculated to be 2.52 eV. The corresponding experimental value is 2.8 eV.[45] In agreement with previous reports,[35,38] the monomer fragmentation energy ($Ag_n \rightarrow Ag_{n-1} + Ag$) shows an odd/even alternation; even clusters are more stable than adjacent odd clusters.

The ground-state isomers for the cationic clusters are reported in the lower part of Figure 1. Upon ionization, the trimer becomes an equilateral triangle. The positively charged tetramer has the same ground-state structure as the neutral counterpart. For the pentamer, the stable isomer is 3D with D_2 symmetry. Also for Ag_6^+, a change in structure as compared with the neutral case is predicted. The stable structure is a planar C_{2v} isomer. A 3D geometry with the same point symmetry group is 0.05 eV higher in energy. The D_{3h} isomer, which is the stable structure for the neutral hexamer, is 0.16 eV higher than the ground state. For the heptamer, a planar isomer with D_{6h} symmetry is calculated to be the stable structure. The pentagonal bi-pyramid, is a meta-stable configuration, which is 0.09 eV higher in energy. For Ag_8^+, the stable structure follows the pentagonal motif present for Ag_7^+ and can be characterized as a pentagonal bi-pyramid with one cap. The bi-capped octahedron and dodecahedron are 0.05 and 0.07 eV, respectively, higher in energy. For the neutral octamer, the T_d isomer is competitive

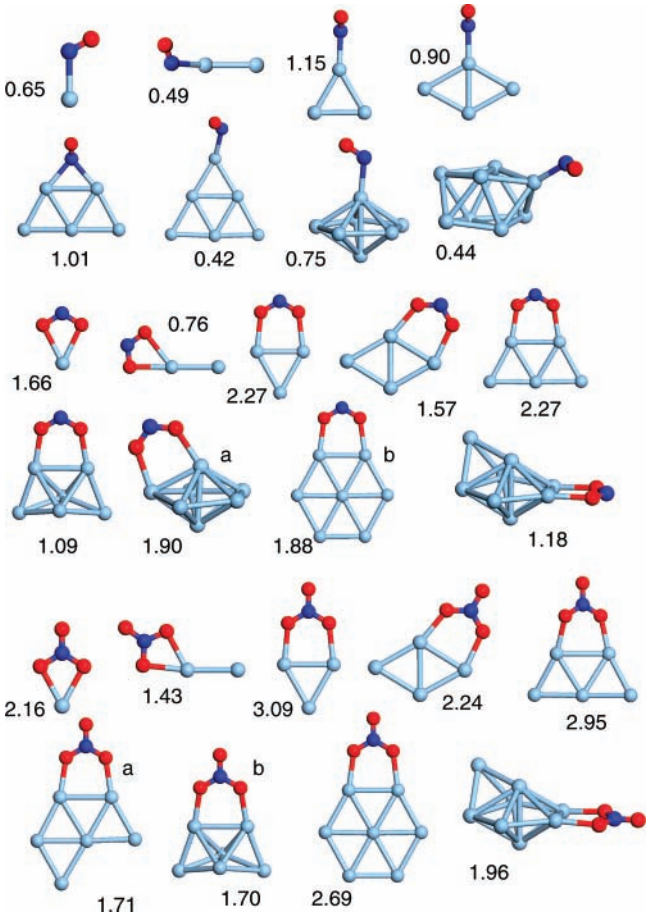

Figure 2. Structural models of NO, NO_2, and NO_3 adsorbed on Ag_n. Two isomers (a and b) are reported for Ag_7NO_2 and Ag_6NO_3, respectively. The corresponding adsorption energies with respect to ground state Ag_n structures and the gas-phase adsorbates are reported in eV. Atomic color code: silver (blue metal), nitrogen (blue), and oxygen (red).

in energy. However, as a cation this isomer is calculated to be meta-stable by 0.46 eV.

From the stable neutral and cationic clusters, the adiabatic ionization potentials (AIP) have been evaluated. These are in eV: 7.78, 5.77, 6.46, 5.89, 6.73, 5.57, and 6.22 for Ag_2 to Ag_8, respectively. Thus, there is marked odd/even alternation also in this electronic property.

B. NO_x Adsorption on Ag_n. We turn now to the issue of NO_x adsorption on Ag_n. First, the geometrical structures are presented together with the size evolution of the adsorption energies. Thereafter, the electronic structure is analyzed in some detail, and finally, the results are presented for vibrational properties.

1. Structural and Energetic Properties. At the top of Figure 2, the stable structures for Ag_nNO are reported. The cluster size dependence of the adsorption energy is shown in Figure 3.

Generally, NO prefers adsorption in an atop configuration. In this geometry, the Ag_n−NO and N−O distances are about 2.17 and 1.18 Å, respectively. The Ag−N−O angle is ∼130°. For the gas-phase NO, the N−O distance is calculated to be 1.15 Å. The HOMO[46] level of NO is the antibonding $2\pi^*$ state. As NO is adsorbed, $2\pi^*$ gets slightly occupied, which rationalizes the elongation of the NO distance as well as the bent adsorption structure. The difference between the singlet and triplet states for the odd Ag_nNO systems is fairly small (within 0.2 eV). AgNO and Ag_7NO are calculated to be singlets,

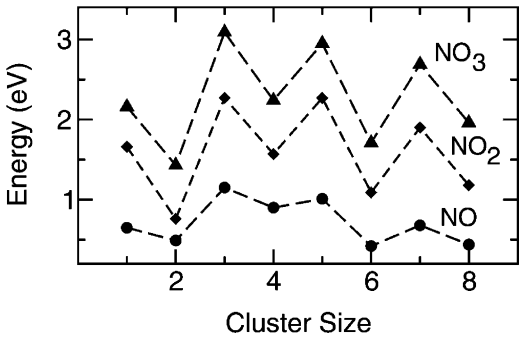

Figure 3. Adsorption energies of NO, NO_2, and NO_3 on Ag_n.

whereas the triplet state is preferred for Ag_3NO and Ag_5NO. The similar stability of the two spin states is most likely related to the low electronic affinity of NO.

Regarding the adsorption site, Ag_5NO is an exception. For this cluster size, NO is adsorbed in a bridge configuration with Ag−N and N−O distances of 2.27 and 1.21 Å, respectively. The underlying reason for the bridge preference on Ag_5 is the electronic structure of the bare cluster. In this case, the HOMO level is a bonding orbital between the two Ag atoms connected to NO. This orbital interacts efficiently with the singly occupied $2\pi^*$ of NO. The long N−O distance is a signature of this interaction.

The calculations do not predict any marked structural relaxations of Ag_n upon NO adsorption. In all cases, the low-energy structures of Ag_n NO are related to the ground-state isomers of Ag_n. However, in the case of Ag_8NO, the preference between the dodecahedron (D_{2d}) and the tetra-capped tetrahedron (T_d) is reversed. With NO adsorbed, the D_{2d} isomer is preferred by 0.05 eV over T_d. The minor structural relaxations signal a weak interaction, which also is calculated. With a clear odd/even alternation, the adsorption energy is predicted to be in the range between 0.5 and 1 eV (Figure 3).

Adsorption of NO on Ag_4 has previously been studied using DFT in an implementation based on local basis functions and effective core potentials.[21] The adsorption energy was reported to be 0.89 eV and the N−O distance to be 1.16 Å for the same configuration as the one in Figure 2. This is in very good agreement with the present results of 0.90 eV and 1.17 Å, respectively.

We now consider NO_2 adsorption. With the exception of the monomer and dimer, NO_2 prefers adsorption in a bridge configuration with an Ag−O distance of ∼2.3 Å. For NO_2, the N−O distance is elongated upon adsorption. In the gas-phase, the calculated N−O distance is 1.20 Å. For Ag_nNO_2, the corresponding distance is ∼1.25 Å. Also the O−N−O angle is changed from 134° for the free molecule to ∼120° when NO_2 is adsorbed. In fact, the molecular structure of adsorbed NO_2 is close to what is calculated for the gas-phase nitrite, namely, an N−O distance of 1.28 Å and an O−N−O angle of 115°. Thus, the structural changes signal a bond mechanism with charge transfer from the cluster to NO_2. This conclusion is, furthermore, supported by the cluster relaxations. For Ag_2−Ag_5, the metal structure of Ag_nNO_2 is similar to that of the bare cluster case. However, in the range Ag_6−Ag_8, the clusters adopt structures that are relevant for the Ag_n cations, indicative of a cluster-to-adsorbate charge transfer. For Ag_6, NO_2 drives the transformation from the planar D_{3h} isomer to the 3D C_{2v}. The planar structure with the lowest energy (0.06 eV above the ground state) is for Ag_6NO_2 based on the cationic ground state with C_{2v} symmetry (Figure 1). Regarding the 2D versus 3D preference, NO_2 has the opposite effect on Ag_7, namely, that 2D

isomers are stabilized. In this case, the planar D_{6h} isomer is only 0.02 eV less preferred than the ground-state pentagonal bi-pyramid. Also for Ag_8NO_2, the ground-state structure is based on the cationic cluster structure, which is a capped pentagonal bi-pyramid. Low-energy structures based on relevant neutral cluster structures are at least ~0.1 eV above the ground state.

The structural trends discussed for NO_2 are also relevant for NO_3 adsorption. NO_3 is generally adsorbed in bridge configuration, where the N−O distance is elongated by ~0.04 Å with respect to the gas phase (from 1.24 to 1.28 Å). The increased N−O distance is similar to what is calculated for the gas-phase nitrate. Regarding the Ag_n geometries, the tendency of cation structures is clearer than that for NO_2. For Ag_6NO_3, the 2D and 3D structures are essentially degenerated. In the case of Ag_7NO_3, the 2D structure is preferred over the pentagonal pyramid by 0.11 eV. The difference between NO_2 and NO_3 correlates with the large difference in electronic affinity (EA). For NO_2, the calculated adiabatic EA is 1.67 eV, whereas the corresponding value is 3.36 eV for NO_3. Thus, it is reasonable that the tendency toward cation structures should be more pronounced for NO_3 adsorption.

The NO, NO_2, and NO_3 adsorption energies are collected in Figure 3. NO_3 is clearly more strongly adsorbed than NO_2, and NO has the lowest adsorption energy. Particularly for NO_2 and NO_3, there is a pronounced odd/even alternation. In several cases, the adsorption energy changed in the order of 1 eV from one cluster size to another. Starting with the trimer, the marked changes correlate with differences in the ionization potential of the clusters. The changes in the adiabatic ionization potential (AIP) are calculated to be $[AIP(Ag_n) - AIP(Ag_{n-1})]$ −2.0, 0.7, −0.6, 0.8, −1.2, 0.6 eV for $n = 3-8$. For NO_3 adsorption on Ag_3 to Ag_8, the differences in adsorption energies $[E_a(Ag_n) - E_a(Ag_{n-1})]$ are 3.1, −0.8, 0.7, −1.2, 1.0, and −0.7 eV, respectively.

2. Analysis of the Electronic Structure. The electronic structure of small Ag_n clusters have been analyzed previously.[9] States close to the HOMO level are of 5s character and are separated from the 4d electrons, which are well below the highest occupied states. The 5s-derived states are delocalized over the cluster. This results in a jellium nature of Ag_n clusters with clear electronic shell closings and a marked odd/even alternation in properties connected to the electronic structure.

Also for NO_x adsorption, the properties of Ag_n clusters are dominated by the 5s electrons. To analyze the bond in detail, the examples with NO and NO_3 on Ag_4 are considered. Ag_4 is chosen because the same cluster isomer is relevant for the bare cluster and the cluster with adsorbates. Because the nature of the NO_2 and NO_3 bond is similar, the discussion is restricted to the latter.

In Figure 4, the electronic density of states (EDOS) for Ag_4, Ag_4NO, and Ag_4NO_3 are reported. For the bare cluster, the center of the d-derived states are localized at −7.5 eV. The spin-degenerated state at the upper edge of the d-band is the fully symmetric combination of 5s-derived states. The HOMO level is a 5s-derived state with a node at a symmetry plane. The LUMO[46] level is a similar type of state but with a perpendicular nodal plane. In the language of jellium clusters, the fully symmetric state corresponds to 1s, whereas the HOMO and LUMO are 1p states.

For Ag_4NO, states mainly located at NO determine the character of the orbitals near the HOMO level. The HOMO level as well as the three first unoccupied states are of $2\pi^*$ character. The molecular 1π and 5σ are centered at −12.2 and −11.4 eV,

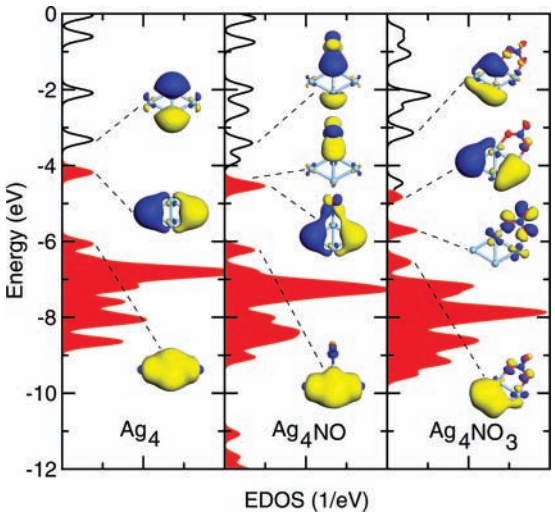

Figure 4. Electronic density of states (DOS) for Ag_4 (left panel), Ag_4NO (middle panel), and Ag_4NO_3 (right panel). The DOS is obtained by a 0.1-eV Gaussian broadening of the one-electron Kohn−Sham energies. Some selected Kohn−Sham orbitals are shown at an isosurface of ± 0.03 1/Å^3.

respectively. The occupied metal states are hybridized with the NO orbitals in a minor fashion. The small effect of NO on the occupied orbitals correlates with the fairly weak interaction between NO and Ag_n.

NO_3 is found to have large effects on the electronic structure of Ag_4. The 1s orbital is clearly affected by the adsorbates and polarized away from NO_3. The state at −5.7 eV is mainly located at the adsorbate. In fact, this orbital corresponds to the HOMO level of NO_3, which in the gas phase is singly occupied. However, in this case, the resonance has two electrons. This is another clear signature of nitrate formation, that is, transfer of one electron from the metal to the adsorbate. The HOMO level is now the singly occupied 1p state. The spin-down counterpart of this orbital is LUMO. The LUMO+1 state resembles the nature of another 1p state.

3. Vibrational Analysis. Vibrational infrared (IR) spectroscopy is a powerful technique that can be used *in situ* to probe the molecular species present in catalytic reactions. Because the mode of vibration is a signature of the potential energy surface experienced by the molecule, such measurements can reveal information on adsorption configuration and bond strengths.

In the present study, the method of finite differences was utilized to calculate the vibrational spectrum for NO, NO_2, and NO_3 adsorbed on Ag_n. For each cluster size, results for the stable adsorption configuration are reported in Figure 5. Although the complete spectra were evaluated, here the discussion is restricted to modes that correspond to internal adsorbate vibrations. The internal metal modes are below 200 cm^{-1}.

In the gas-phase, the wavenumber of the NO stretch vibration is calculated to be 1932 cm^{-1}. This is only a slight overestimation compared with the experimental value[43] of 1904 cm^{-1}. The stretch vibration is clearly softened upon adsorption (lower panel of Figure 5). With the exception of Ag_5, the NO stretch vibration is around 1700 cm^{-1} for all investigated clusters. Just as for the adsorption energy, there is a slight odd−even alternation. The stretch vibration for NO adsorbed on even clusters are higher than that on the adjacent odd clusters. The low wavenumber (1545 cm^{-1}) predicted for Ag_5 is owing to the bridging adsorption configuration for this cluster size. In this geometry, the HOMO of the cluster is efficiently interacting with the $2\pi^*$ orbital of NO, which results in a low stretch vibration. It clearly

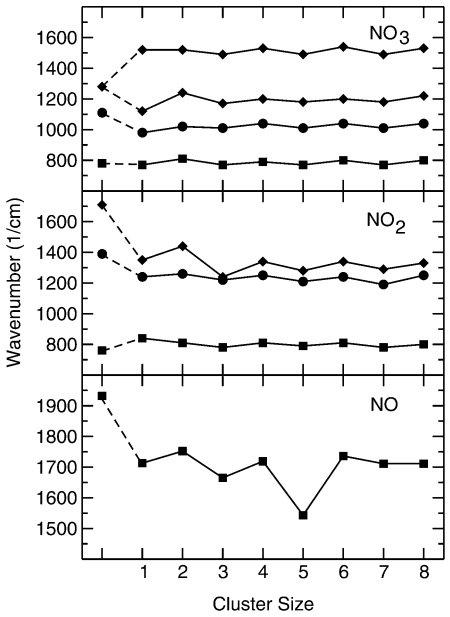

Figure 5. Calculated wavenumbers for NO, NO_2, and NO_3 adsorbed on Ag_n. The values to the left correspond to the calculated molecular gas-phase value.

correlates with the long intermolecular distance (1.21 Å) calculated for NO in this case.

The NO stretch vibration has been measured for neon matrix-isolated AgNO[47] to be 1707 cm^{-1}. This is in good agreement with the present result for AgNO of 1713 cm^{-1}. In ref 21, the NO stretch vibration on Ag_4NO was calculated to be 1873 cm^{-1}, which is clearly higher than our result of 1719 cm^{-1}. However, the vibrational shifts with respect to the gas-phase NO are comparable (~200 cm^{-1}). In ref 21, the vibration of gas-phase NO was reported to be 2076 cm^{-1}.

For NO_2, the wavenumbers for the asymmetric and symmetric stretch vibrations, together with the bend mode, are calculated to be 1710, 1390, and 760 cm^{-1}, respectively. The corresponding experimental values[48] are 1618, 1318, and 750 cm^{-1}. The cluster-size dependence of these modes are reported in the middle panel of Figure 5. The main character of the NO_2 LUMO level is a node between nitrogen and the two oxygen atoms in conjugation with an O−O bond. This character makes the asymmetric NO_2 stretch vibration sensitive to charging. Consequently, it is not surprising that the wavenumber corresponding to this mode is red-shifted by ~400 cm^{-1} for NO_2 adsorbed on Ag_n as compared to the gas-phase NO_2. The symmetric vibration is also shifted to lower wavenumbers by ~200 cm^{-1}. In agreement with the character of the NO_2 LUMO level, the bending mode is instead slightly shifted to higher energies by ~40 cm^{-1}. The odd/even alternation present for the adsorption energies are also reflected in the vibrational signatures. In the gas phase, the bend and asymmetric stretch vibrations are IR active. Of the two modes, the asymmetric stretch is by far the most intense. When NO_2 is adsorbed on Ag_n, the symmetric stretch vibration is also predicted to be IR active. Given the adsorption structure, this is not surprising. The intensities of the symmetric and asymmetric modes are calculated to be of similar strengths (~300 km/mol).

The NO_3 case is reported in the top panel of Figure 5. Three vibrational modes are reported, namely, the out of plane, the symmetric N−O stretch, and the asymmetric N−O stretch, of which the asymmetric stretch is doubly degenerated in the gas-phase. The wavenumbers for these modes are calculated to be 780, 1110, and 1280 cm^{-1}, respectively. The corresponding experimental values[49] are 762, 1060, and 1492 cm^{-1}. As NO_3 is adsorbed, the degeneracy is broken for the asymmetric vibration. The two modes are separated by about 300 cm^{-1} for all cluster sizes. The symmetric mode is softened upon adsorption by ~100 cm^{-1}. Because the out of plane mode does not include motion in the direction toward the cluster, the wave number is calculated to be fairly unchanged upon adsorption. All of the vibrational modes show the same odd/even alternations as a function of cluster size as already discussed for NO and NO_2. The symmetric mode of NO_3 in the gas-phase is not IR active. However, similar to the symmetric mode of NO_2, it becomes active (~100 km/mol) as NO_3 is adsorbed on Ag_n. The mode with the highest wavenumber of the two asymmetric vibrations is the most intense in the spectrum at ~600 km/mol, whereas the asymmetric mode with the lowest wavenumber has an intensity of ~300 km/mol.

IV. Conclusions

Density functional theory was used to explore NO_x adsorption on Ag_n in the range from the monomer to the octamer. NO is found to interact weakly with Ag_n and is preferably adsorbed in an atop configuration. In contrast, NO_2 and NO_3 are adsorbed in a bridge configuration. The adsorption energy between the molecules and the clusters follows the trend $E_a(NO) < E_a(NO_2) < E_a(NO_3)$. Both NO_2 and NO_3 are bonded via charge transfer from the metal to the molecule. This charge transfer has a pronounced effect on the structure of the cluster. In general, isomers relevant for the cationic Ag_n become energetically preferred. Marked odd/even effects dominate the size evolution of electronic properties of Ag_n in the studied size regime. Consequently, odd/even alternations are present in adsorption energies as well as the evaluated vibrational spectra.

Recently, small silver clusters have been suggested to constitute the active phase in Ag/Al_2O_3 catalysts for SCR with HC.[12,13] Given the large size variations in cluster properties, it will be important to investigate whether Ag_n, also supported, shows such marked size variations. One may speculate that either the support reduces the size variation or the functionality of the Ag/Al_2O_3 catalyst is based on clusters with atomic resolution.

Acknowledgment. The Competence Centre for Catalysis is hosted by Chalmers University of Technology and financially supported by the Swedish Energy Agency and the member companies AB Volvo, Volvo Car Corporation, Scania CV AB, GM Powertrain Sweden AB, Haldor Topsoe A/S, and The Swedish Space Agency. This work was supported in part by the Swedish Research Council.

References and Notes

(1) Geusic, M. E.; Morse, M. D.; Smalley, R. E. *J. Chem. Phys.* **1985**, *82*, 590.
(2) Richtsmeier, S. C.; Parks, E. R.; Liu, K.; Pobo, L. G.; Riley, S. J. *J. Chem. Phys.* **1985**, *82*, 3659.
(3) Whetten, R. L.; Cox, D. M.; Trevor, D. J.; Kaldor, A. *Phys. Rev. Lett.* **1985**, *54*, 1494.
(4) Knickelbein, M. B. *Annu. Rev. Phys. Chem.* **1999**, *50*, 79.
(5) Shi, Y.; Ervin, K. M. *J. Chem. Phys.* **1998**, *108*, 1757.
(6) Andersson, M.; Rosen, A. *J. Chem. Phys.* **2003**, *117*, 7051.
(7) Taylor, K. J.; Pettiette-Hall, C. L.; Cheshnovsky, O.; Smalley, R. E. *J. Phys. Chem.* **1991**, *96*, 3319.
(8) Brack, M. *Rev. Mod. Phys.* **1993**, *65*, 677.
(9) Grönbeck, H.; Rosen, A. *Z. Phys. D: At., Mol. Clusters* **1996**, *36*, 153.
(10) Berhardt, T. M. *Int. J. Mass Spectrom.* **2005**, *243*, 1.
(11) Burch, R. *Catal. Rev.* **2005**, *46*, 271.

(12) Sazama, P.; Capek, L.; Drobna, H.; Sobalik, Z.; Dedecek, J.; Arve, K.; Wichterlova, B. *J. Catal.* **2005**, *232*, 302.
(13) Breen, J. P.; Burch, R.; Hardacre, C.; Hill, C. J. *J. Phys. Chem. B* **2005**, *109*, 4805.
(14) Hammer, B. *Phys. Rev. Lett.* **2002**, *89*, 016102.
(15) Molina, L. M.; Hammer, B. *Phys. Rev. Lett.* **2003**, *90*, 206102.
(16) Grönbeck, H.; Broqvist, P. *J. Phys. Chem. B* **2003**, *107*, 12239.
(17) Grönbeck, H. *J. Phys. Chem. B* **2006**, *110*, 11977.
(18) Duarte, H.; Salahub, D. R. *Top. Catal.* **1999**, *9*, 123.
(19) Gutsev, G.; Mochena, M. D.; Johnson, E.; Bauschlicher, C. W. *J. Chem. Phys.* **2006**, *125*, 194312.
(20) Harding, D.; Mackenzie, S. R.; Walsh, T. R. *J. Phys. Chem. B* **2006**, *110*, 18272.
(21) Matulis, V. E.; Ivaskevish, O. A. *Comput. Mater. Sci.* **2006**, *35*, 268.
(22) Hohenberg, P.; Kohn, W. *Phys. Rev.* **1964**, *136*, 864.
(23) Kohn, W.; Sham, L. J. *Phys. Rev.* **1965**, *140*, A1133.
(24) Perdew, J.; Burke, K.; Ernzerhof, M. *Phys. Rev. Lett.* **1996**, *77*, 3865.
(25) Delley, B. *J. Chem. Phys.* **1990**, *92*, 508.
(26) Delley, B. *J. Chem. Phys.* **2000**, *113*, 7756.
(27) We have used DMol, version 4.0.
(28) Delley, B. *Phys. Rev. B* **2002**, *66*, 155125.
(29) Monkhorst, H. J.; Pack, J. D. *Phys. Rev. B* **1976**, *13*, 5188.
(30) Pack, J. D.; Monkhorst, H. J. *Phys. Rev. B* **1977**, *16*, 1748.
(31) Bonacic-Koutecky, V.; Cespiva, L.; Fantucci, P.; Koutecky, J. *J. Phys. Chem.* **1993**, *98*, 7981.
(32) Bonacic-Koutecky, V.; Pittner, J.; Boiron, M.; Fantucci, P. *J. Phys. Chem.* **1999**, *110*, 3876.
(33) Chan, W. T.; Fournier, R. *Chem. Phys. Lett.* **1999**, *315*, 257.
(34) Liu, Z. F.; Yim, W. L.; Tse, J. S.; Hafner, J. *Eur. Phys. J. D* **2000**, *10*, 105.
(35) Fournier, R. *J. Chem. Phys.* **2001**, *115*, 2165.
(36) Weis, P.; Bierweiler, T.; Gilb, S.; Kappes, M. M. *Chem. Phys. Lett.* **2002**, *355*, 355.
(37) Chretien, S.; Gordon, M. S.; Metiu, H. *J. Chem. Phys.* **2004**, *121*, 9925.
(38) Fernandez, E. M.; Soler, J. M.; Garzon, I. L.; Balbas, L. C. *Phys. Rev. Lett.* **2004**, *70*, 165403.
(39) Tian, Z. M.; Tian, Y.; Wei, W. M.; He, T. J.; Chen, D. M.; Liu, F. C. *Chem. Phys. Lett.* **2006**, *420*, 550.
(40) Häkkinen, H.; Moseler, M.; Landman, U. *Phys. Rev. Lett.* **2002**, *89*, 033401.
(41) Furche, F.; Ahlrichs, R.; Weis, P.; Jacob, C.; Gilb, S.; Bierweiler, T.; Kappes, M. M. *J. Chem. Phys.* **2002**, *117*, 6982.
(42) Grönbeck, H.; Broqvist, P. *Phys. Rev. B*, **2005**, *71*, 073408.
(43) *Constants of Diatomic Molecules*; Huber, K. P., Herzberg, G., Eds.; Van Norstrand−Reinholt, New York, 1979.
(44) Simard, B.; Hackett, P. A. *Chem. Phys. Lett.* **1991**, *186*, 415.
(45) *American Institute of Physics Handbook*; McGraw-Hill, New York, 1979.
(46) HOMO: Highest occupied molecular orbital. LUMO: Lowest unoccupied molecular orbital.
(47) Andrews, L.; Citra, A. *Chem. Rev.* **2002**, *102*, 885.
(48) *Handbook of Chemistry and Physics*, 71st ed.; Lide, D. R., Ed.; CRC Press, Inc., Boca Raton, FL, 1990−1991.
(49) Friedl, R. R.; Sander, S. P. *J. Phys. Chem.* **1987**, *91*, 2721.